37. Roth, K. A. & Gordon, J. I. Spatial differentiation of the intestinal epithelium: analysis of enteroendocrine cells containing immunoreactive serotonin, secretin, and substance P in normal and transgenic mice. *Proc. Natl Acad. Sci. USA* **87,** 6408–6412 (1990).
38. Hedrick, L. *et al.* The DCC gene product in cellular differentiation and colorectal tumorigenesis. *Genes Dev.* **8,** 1174–1183 (1994).
39. Bry, L. *et al.* Paneth cell differentiation in the developing intestine of normal and transgenic mice. *Proc. Natl Acad. Sci. USA* **91,** 10335–10339 (1994).
40. Louvard, D., Kedinger, M. & Hauri, H. P. The differentiating intestinal epithelial cell: establishment and maintenance of functions through interactions between cellular structures. *Annu. Rev. Cell Biol.* **8,** 157–195 (1992).
41. Schmidt, G. H., Winton, D. J. & Ponder, B. A. Development of the pattern of cell renewal in the crypt-villus unit of chimaeric mouse small intestine. *Development* **103,** 785–790 (1988).
42. Hermiston, M. L., Green, R. P. & Gordon, J. I. Chimeric-transgenic mice represent a powerful tool for studying how the proliferation and differentiation programs of intestinal epithelial cell lineages are regulated. *Proc. Natl Acad. Sci. USA* **90,** 8866–8870 (1993).
43. Hermiston, M. L. & Gordon, J. I. In vivo analysis of cadherin function in the mouse intestinal epithelium: essential roles in adhesion, maintenance of differentiation, and regulation of programmed cell death. *J. Cell Biol.* **129,** 489–506 (1995).
44. Dodd, J., Morton, S. B., Karagogeos, D., Yamamoto, M. & Jessell, T. M. Spatial regulation of axonal glycoprotein expression on subsets of embryonic spinal neurons. *Neuron* **1,** 105–116 (1988).
45. Hohne, M. W., Halatsch, M. E., Kahl, G. F. & Weinel, R. J. Frequent loss of expression of the potential tumor suppressor gene DCC in ductal pancreatic adenocarcinoma. *Cancer Res.* **52,** 2616–2619 (1992).
46. Hahn, S. A. *et al.* DPC4, a candidate tumor suppressor gene at human chromosome 18q21.1. *Science* **271,** 350–353 (1996).
47. Goodman, C. S. The likeness of being: phylogenetically conserved molecular mechanisms of growth cone guidance. *Cell* **78,** 353–356 (1994).
48. Mortensen, R. M., Conner, D. A., Chao, S., Geisterfer-Lowrance, A. A. & Seidman, J. G. Production of homozygous mutant ES cells with a single targeting construct. *Mol. Cell. Biol.* **12,** 2391–2395 (1992).
49. Stoeckli, E. T. & Landmesser, L. T. Axonin-1, Nr-CAM, and Ng-CAM play different roles in the in vivo guidance of chick commissural neurons. *Neuron* **14,** 1165–1179 (1995).
50. Ekstrand, B. C., Mansfield, T. A., Bigner, S. H. & Fearon, E. R. *Dcc* expression is altered by multiple mechanisms in brain tumors. *Oncogene* **11,** 2393–2402 (1995).

Acknowledgements. We thank B. C. Ekstrand and E. Fearon for generating the data in Fig. 1c; B. Vogelstein for providing reagents and for criticisms of the manuscript; T. Serafini for considerable advice on brain anatomy; V. Lee and M. Yamamoto for antibodies; and E. Taylor, D. Shehu and J. Mak for technical assistance. This work was supported in part by grants from the National Institutes of Health to R.A.W., J.I.G., B. Vogelstein and M.T.-L., and by grants to M.T.-L. from the International Spinal Research Trust and the American Paralysis Association. K.K.-M. was supported by the National Defense Medical College, Japan. M.M. is an associate investigator and M.T.-L. is a research professor of the Howard Hughes Medical Institute. R.A.W. is a research professor of the American Cancer Society.

Correspondence and requests for materials should be addressed to R.A.W. (e-mail: weinberg@wi.mit.edu).

Embryonic lethality and radiation hypersensitivity mediated by Rad51 in mice lacking *Brca2*

Shyam K. Sharan*†, Masami Morimatsu‡§‖, Urs Albrecht¶, Dae-Sik Lim‡☆, Eva Regel†, Christopher Dinh*†, Arthur Sands‡, Gregor Eichele¶, Paul Hasty‡ & Allan Bradley*†

* *Howard Hughes Medical Institute,* † *Department of Molecular and Human Genetics,* ¶ *Department of Biochemistry, Baylor College of Medicine, One Baylor Plaza, Houston, Texas 77030, USA*
‡ *Lexicon Genetics Inc., 4000 Research Forest Drive, The Woodlands, Texas 77381, USA*
§ *Department of Molecular Genetics, The University of Texas, M. D. Anderson Cancer Center, 1515 Holcombe Boulevard, Houston, Texas 77030, USA*
‖ *Department of Biomedical Sciences, Graduate School of Veterinary Medicine, Hokkaido University, Sapporo 060, Japan*

Inherited mutations in the human *BRCA2* gene cause about half of the cases of early-onset breast cancer. The embryonic expression pattern of the mouse *Brca2* gene is now defined and an interaction identified of the Brca2 protein with the DNA-repair protein Rad51. Developmental arrest in Brca2-deficient embryos, their radiation sensitivity, and the association of Brca2 with Rad51 indicate that Brca2 may be an essential cofactor in the Rad51-dependent DNA repair of double-strand breaks, thereby explaining the tumour-suppressor function of Brca2.

Individuals with mutations in either the *BRCA1* or *BRCA2* genes have a dominant cancer predisposition[1,2]. Neoplasia appears to be associated with loss of heterozygosity of the non-mutated alleles in tumours that arise in these patients, suggesting that both of these two genes are tumour suppressors. Inherited mutations in *BRCA1* cause breast cancer and ovarian cancer, whereas inherited mutations in *BRCA2* cause mostly breast cancer with a lower risk of ovarian cancer compared to *BRCA1* (refs 1, 3, 4). The *BRCA2* gene encodes a 3,418-amino-acid protein with no significant homology to any known protein[5,6]. The gene has been extensively screened for mutations in breast tumours, and the results indicate that mutations in *BRCA2* are very rare in non-familial primary breast tumours[4–10]. The mouse Brca2 protein consists of 3,328 amino acids and the overall identity between the human and mouse proteins is 58%, although some regions are more highly conserved[11].

The mouse *Brca2* gene is expressed in adult thymus, testis and ovary and in the midgestation embryo[11]. It is also expressed in mammary epithelial cells and appears to be coordinately regulated with *Brca1* expression[12]. Both *Brca1* and *Brca2* are highly expressed in rapidly proliferating cells, with the expression peaking at the G1/S boundary of the cell cycle[12]. This expression profile and the common breast cancer phenotype seen in patients with mutations in these genes suggest that Brca1 and Brca2 may possibly be acting in the same pathway.

Some insight into BRCA1 function was provided by the observation of an association between BRCA1 and HsRad51 (ref. 13). HsRad51 is the human homologue of the *Escherichia coli* protein RecA and of yeast ScRad51, a member of the *RAD52* epistasis group in *Saccharomyces cerevisiae*[14,15]. *ScRad51* and its homologues are key components of the double-strand-break repair pathway, as shown by phenotypic and biochemical analysis[14,16–20]. ScRad51 is also essential for mitotic and meiotic recombination[14,15,21,22]. Mutation of *rad51* in yeast and mammalian cells results in chromosome loss[14,17]. HsRad51 forms foci in S-phase nuclei and these foci are also immunoreactive against anti-BRCA1 antibodies[13]. Moreover, BRCA1 and HsRad51 colocalize in preparations of meiotic chromosomes. HsRad51 coimmunoprecipitates with BRCA1, confirming that these proteins form a complex. The HsRad51–BRCA1 association suggests that BRCA1 participates in Rad51 functions.

We have examined the function of Brca2 in the mouse. Brca2-deficient embryos are normal throughout early pre- and postimplantation development, but development arrests at the same time as the onset of detectable *Brca2* expression after day 6.5 of gestation.

☆ Present address: Department of Pediatric Oncology, Johns Hopkins Hospital, 720 Rutland Av. Ross 345, Baltimore, Maryland 21205, USA.

Embryonic expression of *Brca2* is at least in part associated with rapidly proliferating tissues. We have also defined an interaction between a conserved region of Brca2 and MmRad51 (mouse homologue of Rad51) in a yeast two-hybrid assay. This result was confirmed in mammalian cells and we show that both genes are coexpressed in the embryo. Brca2-deficient embryos were found to be hypersensitive to γ-irradiation. This shows that the Rad51/Brca2 interaction is functionally significant and suggests a mechanism by which *Brca2* might function as a tumour-suppressor gene.

Brca2 targeting and phenotype analysis

We have mutated the *Brca2* locus in mice using embryonic stem cell technology (Fig. 1). A positive/negative selection strategy was applied to disrupt exon 11 by deleting amino acids 626–1,437 (Fig. 1a, c). The targeting vector, pBrca2TV containing the human *Hprt* minigene as the positive-selection marker and the HSV *tk* gene as the negative-selection marker, was electroporated into AB2.2 ES cells (Fig. 1b). Clones carrying the mutant *Brca2* allele, $brca2^{Brdm1}$, were identified by Southern blotting (Fig. 1d). Four of the eight $brca2^{Brdm1}$/+ES cell lines were injected into blastocysts. Most of the chimaeric mice born transmitted the $brca2^{Brdm1}$ allele to their progeny. The heterozygous mice are healthy and fertile. As loss of BRCA2 function in humans results in tumorigenesis, these mice are currently being monitored for development of neoplasia. So far, none of the mice have shown any signs of tumour formation until at least eight months of age.

Six litters from $brca2^{Brdm1}$/+ intercross matings failed to produce any $brca2^{Brdm1}/brca2^{Brdm1}$ offspring, indicating that *Brca2* was essential for embryonic development. To determine the cause and time of embryonic lethality, embryos at various stages of development were dissected from heterozygous females mated to heterozygous males. At E6.5 of development, 16 embryos were histologically examined. All embryos were normal at this stage. However, by E7.5 about 25% ($n = 45$) of the embryos exhibited a mutant phenotype. At this stage of development, normal embryos have undergone primitive-streak formation[23] (Fig. 2a). Mesoderm is produced and cells start to migrate to form anterior mesoderm around the embryonic ectoderm, and in addition migrate into extraembryonic ectoderm to form structures such as amnion, chorion and allantois. In contrast, the mutant class of embryos resemble E6.5 embryos with very little morphologically visible mesoderm (Fig. 2b, c). However, the differentiation of embryonic ectoderm into mesoderm was confirmed by the presence of *Brachyury* gene expression in the posterior end of the mutant embryo (Fig. 3a, b). The embryonic ectoderm of mutant and wild-type embryos consist of a pseudocolumnar layer of cells, with few dividing cells present. The embryos have a well developed layer of extra-embryonic ectoderm. The amniotic cavity forms and amniotic folds consisting of only the extraembryonic

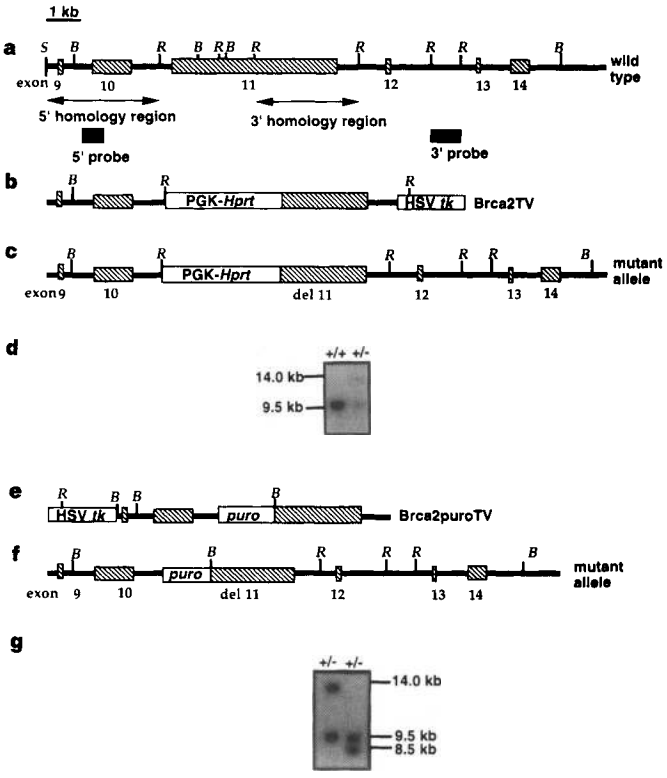

Figure 1 Disruption of *Brca2* gene in ES cells. **a**, Restriction map of the *Brca2* genomic fragment containing exon 9–15 is shown. Restriction sites shown here are *Eco*RI (*R*) and *Bam*HI (*B*). *Sal*I (*S*) is from the cloning vector. Double-headed arrows correspond to the 5′ and 3′ homology regions and the dark shaded boxes show the probes used. **b**, Restriction map of the targeting vector pBrca2TV. **c**, Expected restriction map of the mutated *Brca2* locus. A 2.8-kb genomic region is deleted and replaced by the 3.6-kb *Hprt* gene. **d**, Southern analysis to identify heterozygous ES cells by digesting genomic DNA with *Bam*HI. The 3′ probe detects a 9.5-kb wild-type band and a 14.0-kb mutant band. **e**, Restriction map of the targeting vector pBrca2puroTV electroporated into heterozygous ES cells. A *Bam*HI restriction site was introduced between the *puro* gene and 3′ homology arm. The HSV *tk* gene was ligated to 5′ homology region. **f**, Expected restriction map of the mutant *Brca2* locus. A 2.8-kb genomic region is deleted and replaced by the 1.4-kb *puro* gene. **g**, Southern analysis to identify the second targeting event in heterozygous ES cells by digesting genomic DNA with *Bam*HI. The 3′ probe detects a 9.5-kb wild-type band and a 14.0-kb mutant band. The second targeting results in a 8.5-kb mutant band.

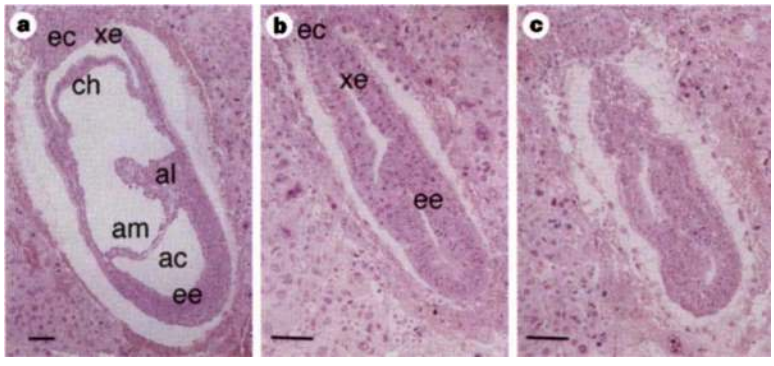

Figure 2 Comparison of *Brca2* mutant embryos with their wild-type littermates. **a**, E7.5 wild-type embryo. **b** and **c**, E7.5 $brca2^{Brdm1}/brca2^{Brdm1}$ embryos. ac, Amniotic cavity; al, allantois; am, amnion; ch, chorion; ec, ectoplacental cone; ee, embryonic ectoderm; xe, extraembryonic ectoderm. Scale bars, 100 μm.

ectoderm layer are evident. In addition to the absence of amnion, mutant embryos completely lack allantois and chorion. However, the visceral and parietal endoderm appear to be normal except for the overall reduction in size.

Brca2 in cell proliferation and survival

The fact that *Brca2* mutant embryos initiate mesoderm formation suggests that the developmental block is not due to lack of differentiation, rather this may result from a proliferation defect. To test this idea, we attempted to generate homozygous mutant ES cells. Given that the developmental block occurred after E6.5 and ES cells are believed to be functionally equivalent to 5.5 day embryonic ectoderm, it should be possible to isolate such cell lines. One of the $brca2^{Brdm1}$/+ES cell clones (D6) was transfected with pBrca2-PuroTV, a targeting vector very similar to the pBrca2TV, except that it had a puromycin gene as the positive-selection marker (Fig. 1e). A total of 12 targeted clones were obtained out of 150 $puro^r$ and $FIAU^r$ cells. However, Southern analysis revealed that none of these 12 clones had disrupted the remaining wild-type *Brca2* allele; instead, all the clones had retargeted the $brca2^{Brdm1}$ allele (Fig. 1g). The failure to obtain any homozygous mutant ES cells is highly significant ($P < 0.01$), which suggests that the *Brca2* gene is required for the survival and/or proliferation of ES cells.

To correlate the expression of *Brca2* with the phenotype seen in *Brca2*-deficient embryos, we examined its expression in embryos using *in situ* hybridization. The mutant phenotype results in an overall developmental arrest which occurs at a time when the entire embryo is undergoing its most rapid phase of cellular proliferation[24,25]. At E6.5 transcripts cannot be detected (Fig. 3c), but at E7.5 the gene is upregulated and expressed throughout the entire embryo, including the extraembryonic tissues (Fig. 3d). No difference in expression levels was detected in the three germ layers. At day E8.5, *Brca2* is expressed in the neuroepithelium and somites, with maximal expression in the migrating neural crest cells that

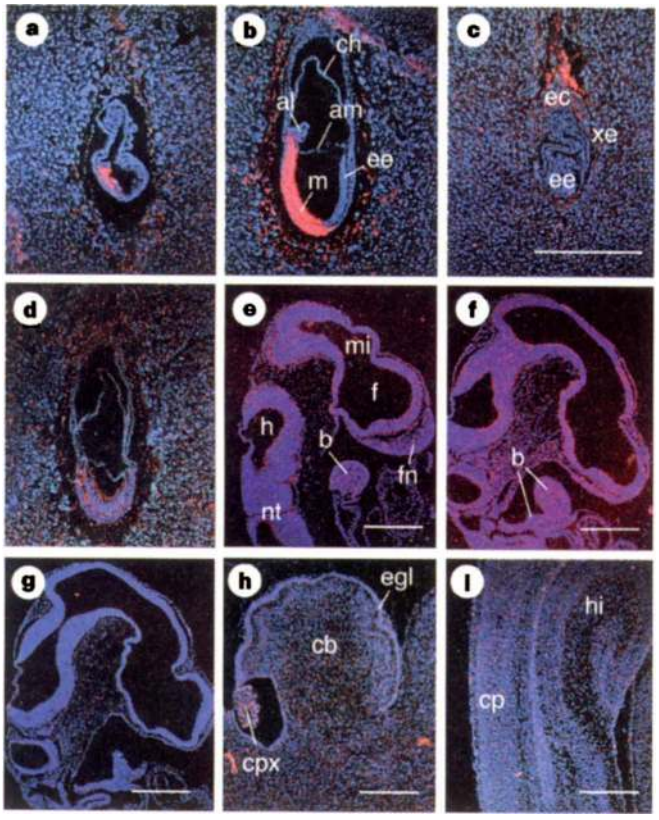

Figure 3 Expression (red signal) of *Brachyury* (*T*) (**a**, **b**) and *Brca2* (**c**–**i**) in the embryos (visualized by Hoechst 33258 DNA stain). **a**, *T* expression is limited to the caudalmost end of a E7.5 $brca2^{Brdm1}$/$brca2^{Brdm1}$ embryo. **b**, E7.5 wild-type embryo showing expresison of *T* extending throughout the posterior mesoderm. **c**, E6.5 wild-type embryo shows no expression of *Brca2*. **d**, E7.5 wild-type embryos with ubiquitous expression. **e**, E9.5 embryo showing broad expression in the entire neuroepithelium and in the frontonasal mesenchyme. **f**, E10.5 embryo illustrating a general upregulation of *Brca2* expression compared to earlier stages. **g**, E10.5 embryo hybridized with sense probe. At birth, cerebellum (**h**) and hypothalamic region (**i**) show no *Brca2* expresison. b, Branchial arches; cb, cerebellum; cp, cortical plate; cpx, choroid plexus; egl, external granular layer; f, forebrain; fn, frontonasal mesenchyme; h, hindbrain; hi, hippocampus; m, mesoderm; mi, midbrain; nt, neural tube; other abbreviations are as in Fig. 2. Scale bars, 500 μm.

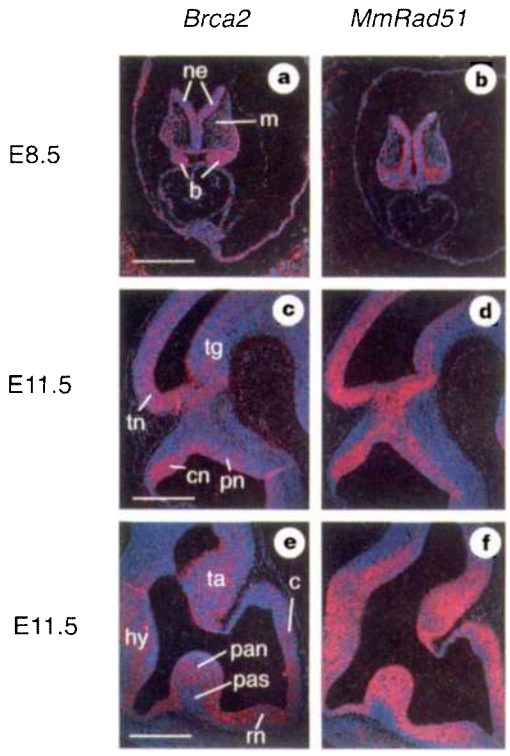

Figure 4 Coexpression of *Brca2* and *MmRad51*. **a**, **c** and **e**, Expression of *Brca2*; **b**, **d** and **f**, expression of *MmRad51*. **a**, **b**, Highly expressed *Brca2* and *MmRad51* in the neural crest cells of an E8.5 embryo which populate the branchial arches and in the neuroepithelium. **c**, **d**, Midbrain–hindbrain boundary of an E11.5 embryo. Strong expresison of both genes is seen in the tectal neuroepithelium, the pontine neuroepithelium and the cerebellar neuroepithelium. Transcripts are less abundant in the tegmental neuroepithelium. **e**, **f**, Forebrain of an E11.5 embryo. Note the lower signal in the non-proliferative pallidal subventricular zone in comparison to the proliferative pallidal neuroepithelium. Expression is also detected in the hypothalamic, thalamic, cortical and rhinencephalic neuroepithelia. Note that the pial surface of the cortical neuroepithelium shows a weaker signal. b, Branchial arches; c, cortical neuroepithelium; cn, cerebellar neuroepithelium; hy, hypothalamic neuroepithelium; m, mesenchyme; ne, neuroepithelium; pan, pallidal neuroepithelium; pas, pallidal subventricular zone; pn, pontine neuroepithelium; rn, rhinencephalic neuroepithelium; ta, thalamic neuroepithelium; tn, tectal neuroepithelium; tg, tegmental neuroepithelium. Scale bars, 500 μm.

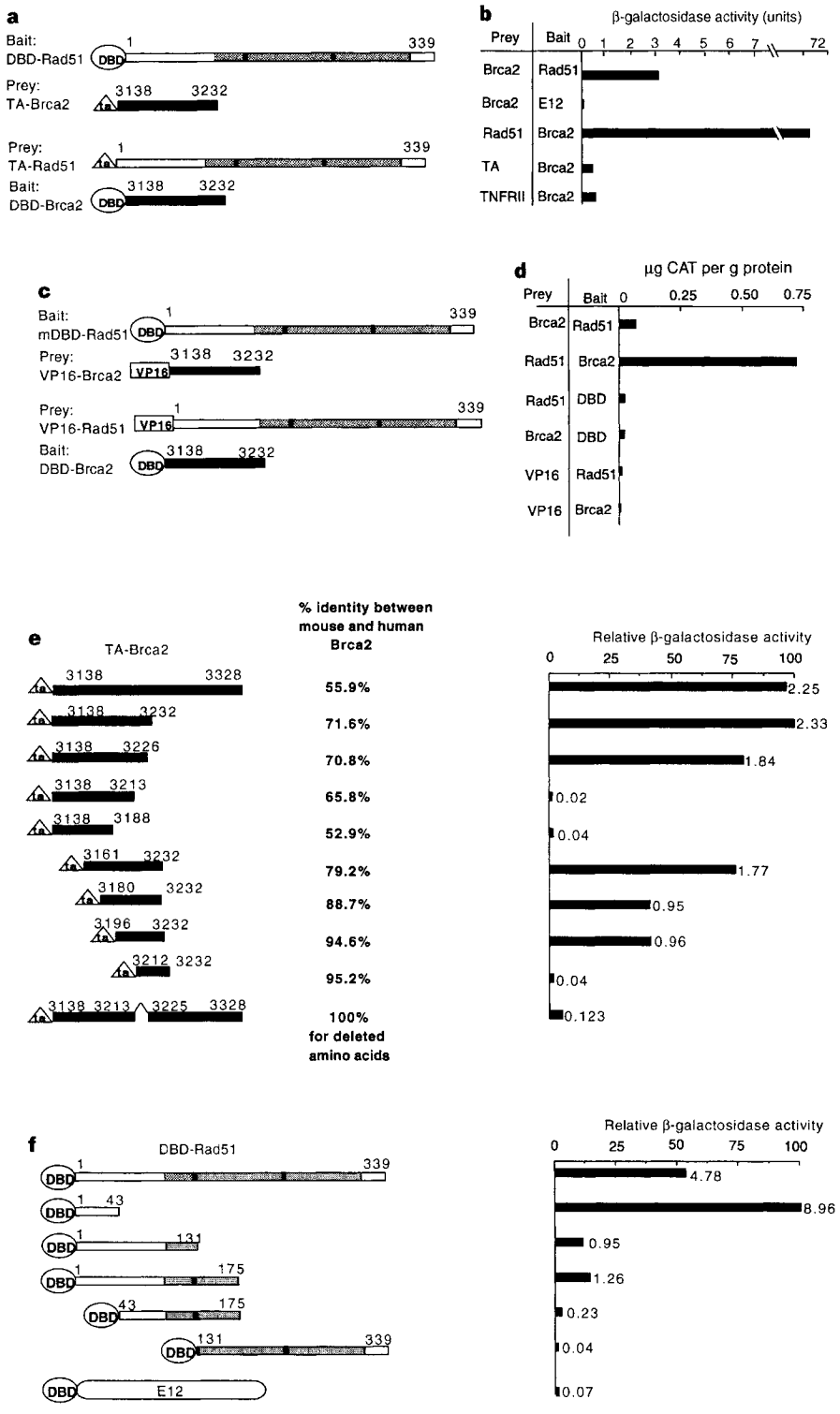

Figure 5 Two-hybrid analysis. **a**, MmRad51-Brca2 interaction in yeast cells. The bait is fused to the *GAL4* DNA-binding domain (DBD) and the prey is fused to the *GAL4* transactivating (TA) domain. MmRad51 (open rectangle) served as both bait, DBD-Rad51 1-339, and prey, TA-Rad51 1-339. Shaded box represents the RecA core homology region[15]. Dark lines represent the conserved ATP-binding motifs. The C-terminal region of Brca2 (filled rectangle) served as both bait, DBD-Brca2 3138-3232 and prey, TA-Brca2 3138-3232. **b**, β-Galactosidase activity in Miller units[46]. E12 is the negative control bait. The transactivating domain of *GAL4* (TA) and tumour-necrosis-factor receptor II (TNFRII) are negative control preys. **c**, MmRad51-Brca2 interaction in mammalian 3T3 cells. The baits were fused to the *GAL4* DNA-binding domain (DBD) and the preys were fused to the activation domain of virion protein 16 (VP16) of herpes simplex virus. MmRad51 served as both bait, mDBD-Rad51 1-339, and prey, VP16-Rad51 1-339. The C-terminal region of Brca2 served as both bait, mDBD-Brca2 3138-3232 and prey, VP16-Brca2 3138-3232. Association of bait and prey were measured by expression of a CAT (chloramphenicol acetyltransferase) gene with a minimal promoter from adenovirus E1b, with five consensus *GLA4* binding sites (pG5 CAT from Clontech). **d**, CAT activity. Negative controls: unfused *GALL4* DNA-binding domain for the bait and unfused VP16 for the prey. **e**, Deletions of *Brca2*. Right, per cent amino-acid identity between mouse and human Brca2. Far right, relative β-galactosidase activity after co-transfection with DBD-Rad51 1-339 as the bait. Miller units are listed at the top of each bar. **f**, Deletion analysis of *MmRad51*. E12 is the negative control bait. Right, relative β-galactosidase activity after co-transfection with TA-Brca2 3138-3328. Miller units are listed at the top of each bar.

populate the branchial arches (Fig. 4a). At E9.5 and E10.5, *Brca2* continues to show a similar spatial expression pattern but there is an overall increase in the level of transcript at E10.5 (Fig. 3e, f). Marked regional differences in expression are first seen by E11.5, at which time transcripts are abundant in the rhinenchephalic, cortical, thalamic, hypothalamic and pallidal neuroepithelium (Fig. 4e), whereas expression in the pallidal subventricular zone and the head mesenchyme (not shown) is decreased. In the midbrain, high concentrations of transcript are detected in the inferior tectal neuroepithelium and these are lower in the superior tectal and tegmental neuroepithelium. In the hindbrain, a strong hybridization signal is seen in the pontine and cerebellar neuroepithelia (Fig. 4c). The gene is also expressed in the dorsal root ganglia and the hepatic primodium (data not shown). At the day of birth, expression in the central nervous system is downregulated to background levels (Fig. 3h, i).

We conclude that *Brca2* expression is transient and largely embryo-specific. It appears that the developmental block occurs when its expression is upregulated at around E7.5. Also, transcripts are particularly prevalent in tissues with a high mitotic index, such as the proliferating ventricular zones of the fore-, mid- and hindbrain, but transcripts are downregulated in post-mitotic cells.

Interaction between Brca2 and Rad51

BRCA1 protein interacts with HsRad51, a protein likely to be involved in the repair of double-strand breaks[13]. In yeast, protein–protein interaction is essential for *ScRad51* function[26]. To identify other proteins that might interact with MmRad51, a yeast two-hybrid screen was done with a T-cell complementary DNA library and a C-terminal region of mouse *Brca2* coding for amino acids 3,138–3,232 was isolated[11] (Genbank accession no. U65594) (Fig. 5a, b). This interaction was directly tested in mammalian cells with similar results (Fig. 5c, d). The association appeared to be much stronger with MmRad51 as the prey and Brca2 as the bait compared with MmRad51 as bait and Brca2 as prey. The possibility that this enhanced interaction was due to transcriptional activity of Brca2 fused to the DNA-binding domain was ruled out because in the absence of MmRad51 as prey, it showed no transactivation (Fig. 5d). This region of Brca2 shows 72% identity with the human homologue[5,6,11]. As the overall identity between the two proteins is 59%, the relatively high degree of conservation in this region suggests that it is functionally significant[11]. A deletion analysis was done on this Brca2 region to determine the amino acids that are critical for the association with MmRad51 (Fig. 5e). Deletions of *Brca2* prey were individually cotransformed into yeast cells with MmRad51 bait and β-galactosidase was assayed. None of the Brca2 deletions interacted with a negative control bait, E12 (not shown). The minimal region that showed a strong association was a 36-amino-acid fragment (residues 3,196–3,232). Deleting 13 of these amino acids (residues 3,213–3,226) ablated the interaction. Note, however, that these 13 amino acids may not be directly involved in Brca2–MmRad51 interaction as the absence of these amino acids may alter the folding of the mutant protein and thus prevent the two proteins from binding. The 36 and 13 amino acids are 95% and 100% conserved, respectively, between mouse and human Brca2, suggesting that this region has a critical function.

A deletion analysis was also done with the MmRad51 bait to determine the region critical for the association with Brca2. The N-terminal region of MmRad51 (amino acids 1–43), but not the C-terminal region, was essential for the interaction (Fig. 5f). The N-terminal region is also responsible for ScRad51–protein associations in *S. cerevisiae*[26], suggesting that this region has a conserved function from yeast to mammals.

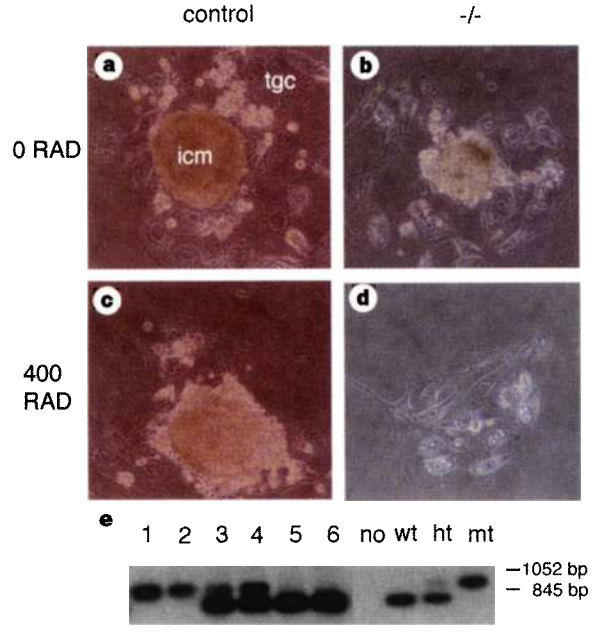

Figure 6 Results of *in vitro* culture of blastocysts after exposure to 400 Rads of γ-radiation. Blastocysts were observed after 7 days in culture. **a**, Unirradiated control blastocyst; **b**, unirradiated mutant blastocyst; **c**, radiated control; and **d**, radiated mutant blastocyst. **e**, Genotyping of blastocysts. Lanes: 1, 2, homozygous mutant; 3, 4, heterozygous; 5, 6, wild type; next four lanes are controls: no, no DNA; wt, wild-type AB2.2 DNA; het, heterozygous ES cell (D6) DNA; met, pBrca2TV DNA. icm, Inner cell mass; tgc, trophoblast giant cells. Scale bars, 120 μm.

Hypersensitivity to γ-irradiation

Mmrad51 and *Brca2* homozygous mutants arrest development at a similar developmental stage and the gene products interact[17] (see above). If Brca2 and MmRad51 interact with each other in the embryo then they should be comparably expressed. The expression pattern of the two genes was found to be almost identical (Fig. 4). Both genes are expressed in rapidly dividing cells and are down-regulated in non-dividing cells.

MmRad51 homozygous mutant embryos are hypersensitive to ionizing radiation[17]. This phenotype should be seen in *Brca2* mutants if the Brca2/Rad51 association has functional significance. Given that it was not possible to make $brca2^{Brdm1}/brca2^{Brdm1}$ cell lines, $brca2^{Brdm1}/brca2^{Brdm1}$ and control (+/+, $brca2^{Brdm1}$/+) E3.5 embryos were investigated for hypersensitivity to γ-radiation. Embryos were obtained from $brca2^{Brdm1}$/+ intercrosses and grown *in vitro* for seven days. Without exposure to radiation, the outgrowth of the inner cellular mass and the number of trophoblast giant cells was equivalent for both mutant and control embryos (Fig. 6a, b). Therefore, inner cell mass outgrowth and trophoblast cell number can be compared for radiation sensitivity. Individual blastocysts were genotyped by PCR (Fig. 6e).

Survival and outgrowth of the inner cell mass was observed for embryos exposed to 400 Rads of γ-radiation. Inner cell mass outgrowth was marginally reduced for eight control (wild-type and heterozygous) embryos after exposure to 400 Rads (Fig. 6c). However, the inner cell mass of $brca2^{Brdm1}/brca2^{Brdm1}$ embryos was totally ablated after 400 Rads in eight out of eight embryos (Fig. 6d). In addition to the inner cell mass outgrowth, γ-radiation reduced the number of trophoblast cells in the homozygous mutants, whereas in cells derived from wild-type and $brca2^{Brdm1}$/+ embryos, there was only a slight decrease in the number of trophoblast cells. In unirradiated control embryos, there was an average of 35 ± 7 trophoblast cells ($n = 13$, whereas irradiated control embryos had 31 ± 5 trophoblast cells ($n = 8$)). However, in the case of $brca2^{Brdm1}/brca2^{Brdm1}$ embryos, the number of trophoblast cells was reduced to 15 ± 3 ($n = 8$).

Discussion

Brca2-deficient embryos suffer an overall developmental arrest after 6.5 days of gestation. This occurs around the time when *Brca2* becomes detectable by *in situ* hybridization analysis. The inability to isolate ES cells homozygous for *Brca2* mutation and the association of embryonic expression of *Brca2* with cells with a high mitotic index is consistent with a *Brca2* function in cell proliferation. This conclusion is supported by studies showing that *Brca2* expression is tightly regulated during mammary epithelial proliferation and differentiation, which is coordinated with *Brca1* expression[12]. Furthermore, *Brca2* is expressed in a cell-cycle-dependent manner and peaks at the G_1/S boundary.

The homozygous mutant phenotype of *Brca2* is similar to that of *Brca1* and *Mmrad51* mutant phenotypes, so these genes may function in similar pathways[17,27,28]. *Brca2*, *Brca1* and *Mmrad51* mutants arrest during development at similar times and homozygous mutant ES cells could not be isolated for any of these genes[17,27,28]. In some respects, the *Brca2* mutant embryos do not show a defect in cell proliferation in *in vitro* cultures of implanting blastocysts (Fig. 6a, b), whereas *Brca1* and *Mmrad51* mutants fail to proliferate[17,27,28]. In addition, *Brca2* mutant embryos initiate mesoderm formation which is absent in *Brca1* and *Mmrad51* mutant embryos. However, radiation sensitivity assays show that *Brca2* mutants, like *Mmrad51* mutants, are hypersensitive to γ-irradiation, implying that the cell-proliferation defect may be secondary to a response to a defect in DNA repair. *Mmrad51* mutant embryos appear to be more sensitive to γ-irradiation than *Brca2* mutants based on the sensitivity of trophoblast cells.

Colocalization and coimmunoprecipitation have shown that human BRCA1 protein interacts with HsRad51 (ref. 13). We have used two-hybrid data from both yeast and mammalian cells to define a mouse Brca2/Rad51 interaction. The stochiometry for this interaction remains to be determined and the existence of additional components or of a conserved mediator in a Brca2/MmRad51 complex cannot be ruled out. The functional significance of this interaction is supported by the similarity of the *Mmrad51* and *Brca2* mutant phenotypes, by the precise coexpression of the two genes, and by the sensitivity of *Brca2* deficient-embryos to γ-irradiation.

This association of Rad51 with Brca1 and Brca2 and the resultant sensitivity of Mmrad51- and Brca2-deficient cells to irradiation may explain the high penetrance of early-onset cancer phenotypes exhibited by patients with either *BRCA1* or *BRCA2* mutations[1,3]. In mammary epithelial cells that have lost BRCA1/2 activity, the HsRad51-mediated DNA-repair functions are presumably compromised, which destabilizes the genome. Rad51 thus serves to suppress tumour formation through interaction with both Brca1 and Brca2. This raises the possibility that *Rad51* might also be a tumour-suppressor gene. In humans, *HsRad51* maps to chromosome 15q15.1, which shows loss of homozygosity in breast tumours[29,30] but no mutation analysis of *HsRad51* in these tumours has been reported.

The role of Brca2 in DNA repair is unknown; it is a very large protein and so could have several functions, including that of a scaffold protein or a matchmaker. This role would be consistent with the greater severity of the *MmRad51* mutation compared with that in *Brca2*; presumably in the absence of Brca2, some Mmrad51 functions can continue, but eventually the auxiliary function of Brca2 becomes limiting. Many proteins and interactions are essential for monitoring and for repairing DNA breaks in conjunction with regulating the cell cycle in response to these breaks[31]. A defect in the repair pathway would lead to cell-cycle arrest or cell death.

Why does *Brca2* deficiency cause cell lethality in early embryos and ES cells, whereas *BRCA2*-deficient mammary epithelial cells proliferate and form tumours? One explanation is that the proliferation arrest is cell-type specific. The embryo and totipotent ES cells are very sensitive to unrepaired breaks and so the cells are not viable. In contrast, *BRCA2*-deficient breast epithelial cells can survive with an unstable genome, but presumably they accumulated genomic alterations that contribute to the malignancy. Taken together, Brca1, Rad51 and Brca2 may be involved in detecting and repairing double-strand breaks, thereby controlling cell-cycle progression. Loss of this repair/monitor system has a direct effect on cell proliferation in the early embryo and tumorigenesis in the adult.

Mouse knockouts of familial tumour-suppressor genes vary in the degree to which they model the human syndrome. In some models, tumours are not observed[27,28,32], in others the tissue spectrum is quite different[33], and others closely reflect the human disease[34–37]. Evidently there are many species-specific factors that contribute to the probability of tumour growth in *Brca2* heterozygous mice. It is too early to define the extent to which *Brca2* heterozygous mice will resemble the susceptibility, penetrance and tissue specificity of the disease in humans. Given the conservation of the Rad51 and the portion of Brca2 involved in the interaction between the two species and the sensitivity of Brca2-deficient cells to γ-irradiation, it is likely that the heterozygous mice will be susceptible to tumours. □

Methods

Construction of *Brca2* targeting vectors. A targeting vector with positive–negative selection designed to delete 2.8 kb of the *Brca2* genomic locus, including the splice acceptor site and 812 amino acids of exon 11. A genomic clone was isolated from a mouse 129SvEv genomic library using a mouse *Brca2* cDNA (Fig. 1a). The targeting vector (pBrca2TV) consisted of a 3.2 kb *Eco*RI–*Sal*I (*Sal*I site from polylinker of phage clone) fragment as the 5′ homology region and a 3.0-kb *Eco*RI fragment representing the 3′ homology region which were ligated to the human PGK–*Hprt* minigene (Fig. 1b). The HSV *tk* gene was ligated downstream of the 3′ homology region. pBrca2-puroTV was constructed similarly to pBrca2TV, except that the puromycin-resistance gene, *puro*, was used as positive-selection marker (Fig. 1e). Electroporation and ES cell culture were done as described[38].

Southern blot analysis to genotype ES cells and mice. To identify the mutant ES cells that were correctly targeted and to genotype the mice, genomic DNA was digested with *Bam*HI and analysed as described[39]. An 800-bp *Eco*RI fragment was used that detects a 9.5-kb fragment in wild-type DNA and 14.0-kb fragment in targeted clones (Fig. 1d). Homologous recombination in the 5′ homology region was confirmed by stripping the blot and rehybridizing with a 400-bp *Rsa*I fragment. The wild-type *Bam*HI fragment detected by this probe is 3.5 kb and the mutant fragment is 14 kb (data not shown). To identify the second targeting event in D6 cells electroporated with pBrca2puroTV, Southern blots of *Bam*HI-digested genomic DNA were hybridized with the 800-bp *Eco*RI fragment. The probe detects a 9.5-kb wild-type fragment, a 14-kb mutant band from the first targeting and a new 8.5-kb mutant fragment from retargeting (Fig. 1g). Mice were generated from ES cells as described[38].

Histological analysis and *in situ* hybridization. Embryos contained inside the decidua were fixed in Bouin's solution and processed for histological analysis as described[23]. Sections were stained with haematoxylin and eosin. *In situ* hybridization was done as described[40]. *Brca2* antisense and sense RNA probes corresponding to the nucleotides 6,887 and 7,249 were used. Hybridization was overnight at 58 °C and washes were at 64 °C. *Brachyury* and *MmRad51* expression were detected as described[15,41].

Yeast and mammalian two-hybrid vectors. Construction of the *MmRad51* bait, DBD–Rad51 1–339: Full-length *MmRAD51* cDNA was amplified by the polymerase chain reaction (PCR) with *pfu* DNA polymerase (Stratagene) using a 5′ sense oligonucleotide with a *Bam*HI site (5′-AAGGATCGATGGATCCTC ATGGCTATGCAAATG-3′) and a 3′ antisense oligonucleotide with a *Kpn*I site (5′-CAGATTCCATGGTACCTTTGGCATCGCC-3′). The amplified PCR fragment was cloned into the bait expression vector pASI (ref. 42).

Deletions of the *MmRAD51* bait. The PCR fragment was digested with *Bam*HI/*Hae*II, *Bam*HI/*Eco*RI, and *Bam*HI/*Nhe*I and cloned into pASI to create DBD–Rad51 1–93, DBD–Rad51 1–131, and DBD–Rad51 1–175, respectively. The other three deletion mutants were made from PCR products generated with *pfu* DNA polymerase using the following primers: DBD–Rad51 1–43, 5′ sense, 5′-CATATGGCCATGGAGATGGCTATGCAAATG-3′, 3′ antisense 5′-GGATCCGTCGACCCACTGTATGGTACCCGG-3′; DBD–Rad51 43–175, 5′

sense 5′-CATATGGCCATGGAGGCTGTTGCTTATGCACGG-3′, 3′ antisense 5′-GGATCCGTCGACTGCTAGCAGCCGCTCCGG-3′; DBD–Rad51 131–339, 5′ sense 5′-CATATGGCCATGGAGTTTGGAGAATTCCGAACT-3′, 3′ antisense 5′-GGATCCGTCGACGAGTCAGTCTTTGGCATC-3′.

Deletions of the *BRCA2* prey. A Brca2 cDNA fragment encoding amino acids 3,138–3,232 was isolated from the yeast two-hybrid screen. TA–Brca2 3138–3328 was obtained by a three-way ligation with pACT cut with *Xho*I–*Hin*dIII, *Brca2* cut with *Xho*I–*Sty*I (from TA–Brca2 3138–3232) and *Brca2* cut with *Sty*I–*Hin*dIII (from a genomic DNA library; extends the original *Brca2* cDNA to the stop codon). From these template DNAs, deletion clones were made by PCR and cloned into the *Xho*I site of pACT. Oligonucleotides used were: TA–Brca2 3138–3226, 5′ sense 5′-CTATCTATTCGATGATGAAGA-3′ (PACTUP for pACT), 3′ antisense, 5′-CACCTCGAGCTCCGTGGCGGCTGAAAAG-3′; TA–Brca2 3138–3213, 5′ sense, PACTUP, 3′ antisense, 5′-CACCTCGAGC TCCGTGGCGGCTGAAAAG-3′; TA–Brca2 3138–3188, 5′ sense, PACTUP, 3′ antisense, 5′-ACAGGTTTTTGGGTCATCAA-3′; TA–Brca2 3161–3232, 5′ sense, 5′-GAAGTCTATGCCCCTGGCTCA-3′, 3′ antisense, 5′-GTGAACTT GCGGGGTTTTTCAGT-3′ (PACTLW for pACT); TA–Brca2 3180–3232, 5′ sense, 5′-GAACGAGATTGATGACCCAA-3′, 3′ antisense, PACTLW; TA–Brca2 3196–3232, 5′ sense, 5′-CACCTCGAGATTTACCTTTCCTAAGTC GG CTGCCCTTA-3′, 3′ antisense, PACTLW; TA–Brca2 3212–3232, 5′ sense, 5′-CACCTCGAGATTTACCCTTTGTCTCTCCAGCTGCACA-3′, 3′ antisense, PACTLW; TA–Brca2 del 3213–3225, template; TA–Brca2 3138–3328, first PCR 5′ part was same as TA-Brca2 3138–3213; for 3′ part, 5′ sense, 5′-TCCCATCTGTACCTTTGTCAGATCTTGTGGCACGAAAT ACGCA-3′, 3′ antisense, PACTLW. These fragments were linked by second PCR with 5′ PACTUP and 3′ PACTLW primers.

To make DBD–Brca2 3138–3232, the *BRCA2* C-terminal region encoding amino acids 3138–3232 was released from TA–Brca2 3138–3232 with *Bgl*II and cloned into the *Bam*HI site of pASI.

Yeast two-hybrid screen. HF7c yeast[43] cells containing DBD–Rad51 were transformed with 400 μg mouse T cell pACT library. MmRad51 interacting clones were identified as described[42,44]. Colonies were tested for specificity by transforming HF7c yeast without bait and with a nonspecific bait, E12. For deletion analysis, the bait and prey were cotransformed and grown in the absence of tryptophan and leucine. β-Galactosidase activity in yeast was assayed as described[45].

Mammalian two-hybrid screen. 3T3 cells were transiently cotransfected with bait, prey and reporter plasmids by lipofection (Lipofectamine, Gibco BRL). Sixty hours later, CAT enzyme was extracted from the cells and measured by ELISA (Boehringer).

***In vitro* culture and radiation treatment of blastocysts.** Blastocysts were isolated at day 3.5 from *brca2*^{Brdm1}/+ females mated to *brca2*^{Brdm1}/+ males (day zero). Blastocysts were exposed to 400 Rads of γ-radiation in a Gammacell 1000 irradiator (1,000 Rads min^{-1}) and cultured in DMEM + 15% FCS-containing medium for 7 days.

PCR genotyping of blastocysts. Blastocysts were picked after washing the plates with PBS and lysing in 20 μl lysis buffer (50 μl KCl, 10 mM Tris HCl, pH 8.3, 2.5 mM $MgCl_2$, 0.01 mg ml^{-1} gelatine, 0.45% Tween 20 and 0.45% NP40) and 2 μl 10 mg ml^{-1} Proteinase K for 4–5 h at 55 °C. Three primers were used in the PCR reaction. A single antisense primer (5′-CCCACTAGCTGTAT-GAAAAC-3′) was designed to amplify both wild-type as well as the mutant band. The first sense primer (5′-GCAAAAAGTAGGACCAAGAGG-3′) was designed from exon 11 to amplify an 845-bp wild-type band and a second sense primer from human *Hprt* minigene (5′-CCCACGAAGTGTTGGATATA-3′) amplified a 1,052-bp mutant band. PCR products were resolved on 1.2% agarose gel. Southern blots were hybridized with [γ-^{32}P]ATP-labelled oligomer (5′-TACTGATTGCTTTCTTGTGA-3′).

Received 13 February; accepted 19 March 1997.

1. Wooster, R. *et al.* Localization of a breast cancer susceptibility gene, *BRCA2*, to chromosome 13q12-13. *Nature* **265,** 2088–2090 (1994).
2. Smith, S. A., Easton, D. G., Evans, D. G. R. & Ponder, B. A. J. Allele losses in the region 17q12-21 in familial breast and ovarian cancer involve the wild type chromosome. *Nature Genet.* **2,** 128–131 (1992).
3. Easton, D. F., Bishop, D. T., Ford, D., Crockford, G. P. & the breast cancer linkage consortium Genetic linkage analysis in the familial breast and ovarian cancer: Results from 214 families. *Am. J. Hum. Genet.* **52,** 678–701 (1993).
4. Gayther, S. A. *et al.* Variations of risks of breast and ovarian cancer associated with different germline mutations of the *BRCA2* gene. *Nature Genet.* **15,** 103–105 (1997).
5. Wooster, R. *et al.* Identification of the breast cancer susceptibility gene *BRCA2*. *Nature* **378,** 789–792 (1995).
6. Tavtigian, S. V. *et al.* The complete *BRCA2* gene and mutations in chromosome 13q-linked kindreds. *Nature Genet.* **12,** 333–337 (1996).
7. Couch, F. J. *et al.* BRCA2 germline mutations in male breast cancer cases and breast cancer families. *Nature Genet.* **13,** 123–125 (1996).
8. Neuhausen, S. *et al.* Recurrent BRCA2617delT mutations in Ashkenazi Jewish women affected by breast cancer. *Nature Genet.* **13,** 126–128 (1996).
9. Phelan, C. M. *et al.* Mutation analysis of the BRCA2 gene in 49 site specific breast cancer families. *Nature Genet.* **13,** 120–122 (1996).
10. Thorlacius, S. *et al.* A single *BRCA2* mutation in male and female breast cancer families from Iceland with varied cancer phenotypes. *Nature Genet.* **13,** 117–119 (1996).
11. Sharan, S. K. & Bradley, A. Murine Brca2: Sequence, map position and expression pattern. *Genomics* **40,** 234–241 (1997).
12. Rajan, J. V., Wang, M., Marquis, S. T. & Chodosh, L. A. *Brca2* is coordinately regulated with *Brca1* during proliferation and differentiation in mammary epithelial cells. *Proc. Natl Acad. Sci. USA* **93,** 13078–13083 (1996).
13. Scully, R. *et al.* Association of BRCA1 with Rad51 in mitotic and meiotic cells. *Cell* **88,** 265–275 (1997).
14. Malkova, A., Ivanov, E. L. & Harber, J. E. Double strand break repair in the absence of RAD51 in yeast: a possible role of break-induced DNA replication. *Proc. Natl Acad. Sci. USA* **93,** 7131–7136 (1996).
15. Shinohara, A. *et al.* Cloning of human, mouse and fission yeast recombination genes homologous to RAD51 and RecA. *Nature Genet.* **4,** 239–243 (1993).
16. Shinohara, A., Ogawa, H. & Ogawa, T. Rad51 protein involved in repair and recombination in *S. cerevisiae* is a RecA-like protein. *Cell* **69,** 457–470 (1992).
17. Lim, D.-S. & Hasty, P. A mutaiton in mouse *rad51* results in an early embryonic lethal that is suppressed by a mutation in *p53*. *Mol. Cell. Biol.* **16,** 7133–7143 (1996).
18. Sung, P. & Robberson, D. L. DNA strand exchange mediated by a Rad51-ssDNA nucleoprotein filament with polarity opposite to that of RecA. *Cell* **82,** 453–461 (1995).
19. Raddling, C. M. Helical interactions in homologous pairing and strand exchange driven by RecA protein. *J. Biol. Chem.* **266,** 5355–5358 (1991).
20. Baumann, P., Benson, F. E. & West, S. C. Human Rad51 protein promotes ATP-dependent homologous pairing and strand transfer reactions *in vitro*. *Cell* **87,** 757–766 (1996).
21. Bishop, D. K. RecA homologs Dmc1 and rad51 interact to form multiple nuclear complexes prior to meiotic chromosome synapsis. *Cell* **79,** 1081–1092 (1994).
22. Rockmill, B., Sym, M., Scherthan, H. & Roeder, G. S. Role of two RecA homologs in promoting meiotic chromosome synapsis. *Genes Dev.* **9,** 2684–2695 (1995).
23. Kaufman, M. H. in *The Atlas of Mouse Development* 2–5 (Academic, San Diego, 1992).
24. Snow, M. L. H. Gastrulation in the mouse: Growth and regionalization of the epiblast. *J. Embryol. Exp. Morph.* **42,** 293–303 (1977).
25. Power, M.-A. & Tam, P. P. L. Onset of gastrulation, morphogenesis and somitogenesis in mouse embryos displaying compensatory growth. *Anat. Embryol.* **187,** 493–504 (1993).
26. Donovan, J. W., Milne, C. T. & Weaver, T. D. Homotypic and heterotypic protein associations control Rad51 function in double-strand break repair. *Genes Dev.* **8,** 2552–2562 (1994).
27. Hakem, R. *et al.* The tumor suppressor gene Brca1 is required for embryonic cellular proliferation in the mouse. *Cell* **85,** 1009–1023 (1996).
28. Liu, C. Y., Flesken-Nikitin, A., Li, S., Zeng, Y. & Lee W.-H. Inactivation of the mouse *Brca1* gene leads to failure in the morphogenesis of the egg cylinder in early postimplantation development. *Genes Dev.* **10,** 1835–1843 (1996).
29. Devilee, P. *et al.* Allelotype of human breast carcinoma: a second major site for loss of heterozygosity is on chromosome 6q. *Oncogene* **6,** 1705–1711 (1991).
30. Wick, W. *et al.* Evidence for a novel tumor suppressor gene on chromosome 15 associated with progression to a metastic stage in breast cancer. *Oncogene* **12,** 973–978 (1996).
31. Carr, A. M. & Hoekstra, M. F. The cellular response to DNA damage. *Trends Cell Biol.* **5,** 32–40 (1995).
32. Kreidberg, J. A. *et al.* WT-1 is required for early kidney development. *Cell* **74,** 679–791 (1993).
33. Hu, N. *et al.* Heterozygous *Rb-1 delta20*/+ mice are predisposed to tumors of the pituitary gland with nearly complete penetrance. *Oncogene* **9,** 1021–1027 (1994).
34. Su, L.-K., Vogelstein, B. & Kinzler, K. W. Association of the APC tumor suppressor protein with catenins. *Science* **262,** 1734–1737 (1993).
35. Sands, A. T., Abuin, A., Sanchez, A., Conti, C. J. & Bradley, A. High susceptibility to ultraviolet-induced carcinogenesis in mice lacking *XPC*. *Nature* **377,** 162–165 (1995).
36. de Vries, A. *et al.* Increased susceptibility to ultraviolet B and carcinogenesis of mice lacking the DNA excision repair gene *XPA*. *Nature* **377,** 169–173 (1995).
37. Donehower, L. A. *et al.* Mice deficient for *p53* are normal but susceptible to spontaneous tumours. *Nature* **356,** 215–221 (1992).
38. Matzuk, M. M., Finegold, M. J., Su, J.-G. J., Hsueh, A. J. W. & Bradley, A. α-Inhibin is a tumour-suppressor gene with a gonadal specificity in mice. *Nature* **360,** 313–319 (1992).
39. Ramirez-Solis, R., Davis, A. & Bradley, A. Gene targeting in embryonic stem cells. *Meth. Enzymol.* **225,** 855–878 (1993).
40. Albecht, U., Eichele, G., Helms, J. A. & Lu, H.-C. in *Molecular and Cellular Methods in Developmental Toxicology* (ed. Daston, G. P.) 23–48 (CRC Press, Boca Raton, 1997).
41. Herrmann, B. G. Expression pattern of the *Brcachyury* gene in whole-mount T^{wis}/T^{wis} mutant embryos. *Development* **120,** 913–917 (1991).
42. Durfee, T. *et al.* The retinoblastoma protein associates with the protein phsophatase type 1 catalytic subunit. *Genes Dev.* **7,** 555–569 (1993).
43. Feilotter, H. E., Hannon, G. J., Ruddell, C. J. & Beach, D. Construction of an improved host strain for two hydbrid screening. *Nucleic Acids. Res.* **22,** 1502–1503 (1994).
44. Breeden, L. & K. Nasmyth, K. Regulation of the yeast HO gene. *Cold Spring Harb. Symp. Quant. Biol.* **50,** 643–650 (1985).
45. Guarente, L. Yeast promoters and *lacZ* fusions designed to study expression of cloned genes in yeast. *Meth. Enzymol.* **101,** 181–191 (1983).
46. Miller, J. H. in *Experiments in Molecular Genetics* 352–355 (Cold Spring Harbor Laboratory Press, Cold Spring Harbor, NY, 1972).

Acknowledgements. We thank S. Rivera, J. D. Wallace, A. Benjamin and S. Vaishnav for technical assistance; J. Staudinger for advice on the yeast two-hybrid screen; S. Elledge and E. Olson for the yeast two-hybrid components; D. Beach for the HF7c strain of yeast; and S. Jones and T. Prolla for technical advice and critical review of the manuscript. This research was supported by grants from the NIH (A.B.) and NIH SPORE (G.E.), and the Howard Hughes Medical Institute. A.B. is an Associate Investigator with HHMI.

Correspondence and requests for materials shoudl be addressed to A.B. (Brca2) (e-mail: abradley@bcm.tmc.edu) or P.H. (Rad51) (e-mail: phasty@lexgen.com).